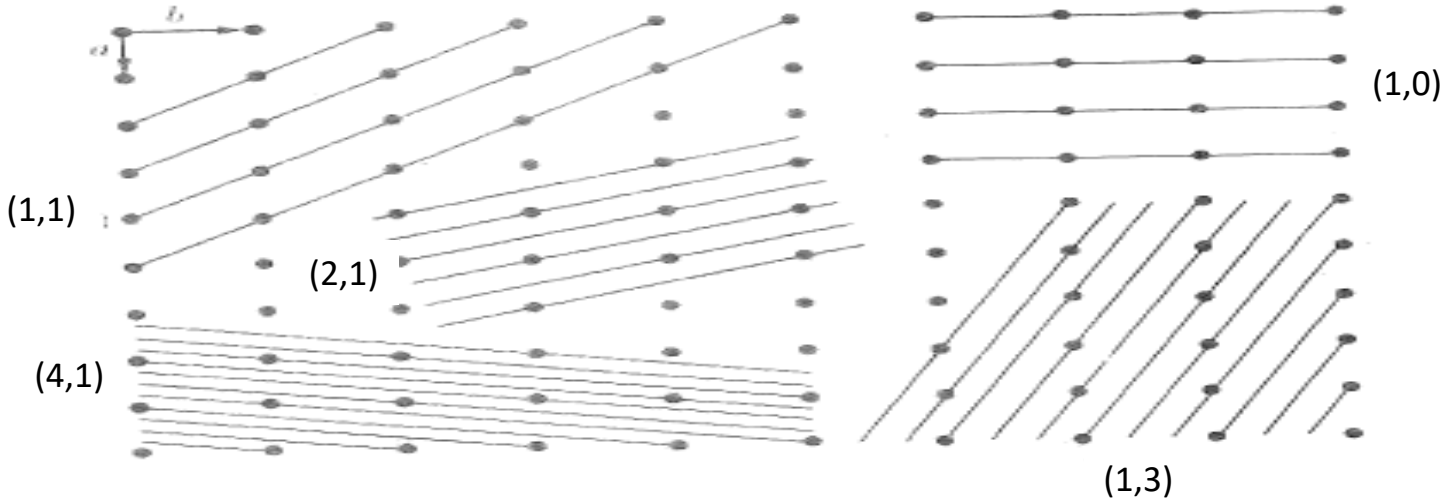
(1,1)
(2,1)
(4,1)
(1,0)
(1,3)

Data Table 30 K_2PtCl_6

Cubic, space group $Fm3m$, No. 225; $a = 9.755$ Å; $Z = 4$, $V = 928.28$ Å^3

Atomic Positions

Pt in 4(a): 0,0,0; fc

Cl in 24(e): $\pm(x,0,0;\ 0,x,0;\ 0,0,x)$; $x = 0.240$; fc

K in 8(c): $\pm\ \frac{1}{4},\frac{1}{4},\frac{1}{4}$; fc

Positions

Multiplicity, Wyckoff letter, Site symmetry			Coordinates			
			(0, 0, 0) +	(0, ½, ½) +	(½, 0, ½) +	(½, ½, 0) +
192	*l*	1	(1) x, y, z (5) z, x, y (9) y, z, x (13) $y, x, \bar{z}$ (17) $x, z, \bar{y}$ (21) $z, y, \bar{x}$ (25) $\bar{x}, \bar{y}, \bar{z}$ (29) $\bar{z}, \bar{x}, \bar{y}$ (33) $\bar{y}, \bar{z}, \bar{x}$ (37) $\bar{y}, \bar{x}, z$ (41) $\bar{x}, \bar{z}, y$ (45) $\bar{z}, \bar{y}, x$	(2) $\bar{x}, \bar{y}, z$ (6) $z, \bar{x}, \bar{y}$ (10) $\bar{y}, z, \bar{x}$ (14) $\bar{y}, \bar{x}, \bar{z}$ (18) $\bar{x}, z, y$ (22) $z, \bar{y}, x$ (26) $x, y, \bar{z}$ (30) $\bar{z}, x, y$ (34) $y, \bar{z}, x$ (38) y, x, z (42) $x, \bar{z}, \bar{y}$ (46) $\bar{z}, y, \bar{x}$	(3) $\bar{x}, y, \bar{z}$ (7) $\bar{z}, \bar{x}, y$ (11) $y, \bar{z}, \bar{x}$ (15) $y, \bar{x}, z$ (19) $\bar{x}, \bar{z}, \bar{y}$ (23) $\bar{z}, y, x$ (27) $x, \bar{y}, z$ (31) $z, x, \bar{y}$ (35) $\bar{y}, z, x$ (39) $\bar{y}, x, \bar{z}$ (43) x, z, y (47) $z, \bar{y}, \bar{x}$	(4) $x, \bar{y}, \bar{z}$ (8) $\bar{z}, x, \bar{y}$ (12) $\bar{y}, \bar{z}, x$ (16) $\bar{y}, x, z$ (20) $x, \bar{z}, y$ (24) $\bar{z}, \bar{y}, \bar{x}$ (28) $\bar{x}, y, z$ (32) $z, \bar{x}, y$ (36) $y, z, \bar{x}$ (40) $y, \bar{x}, \bar{z}$ (44) $\bar{x}, z, \bar{y}$ (48) z, y, x
96	*k*	. .*m*	x, x, z $\bar{x}, \bar{x}, z$ $\bar{x}, x, \bar{z}$ $x, \bar{x}, \bar{z}$ z, x, x $z, \bar{x}, \bar{x}$ $\bar{z}, \bar{x}, x$ $\bar{z}, x, \bar{x}$ x, z, x $\bar{x}, z, \bar{x}$ $x, \bar{z}, \bar{x}$ $\bar{x}, \bar{z}, x$ $x, x, \bar{z}$ $\bar{x}, \bar{x}, \bar{z}$ $x, \bar{x}, z$ $\bar{x}, x, z$ $x, z, \bar{x}$ $\bar{x}, z, x$ $\bar{x}, \bar{z}, \bar{x}$ $x, \bar{z}, x$ $z, x, \bar{x}$ $z, \bar{x}, x$ $\bar{z}, x, x$ $\bar{z}, \bar{x}, \bar{x}$				
96	*j*	*m* . .	$0, y, z$ $0, \bar{y}, z$ $0, y\,\bar{z}$ $0, \bar{y}, \bar{z}$ $z, 0, y$ $z, 0, \bar{y}$ $\bar{z}, 0, y$ $\bar{z}, 0, \bar{y}$ $y, z, 0$ $\bar{y}, z, 0$ $y, \bar{z}, 0$ $\bar{y}, \bar{z}, 0$ $y, 0, \bar{z}$ $\bar{y}, 0, \bar{z}$ $y, 0, z$ $\bar{y}, 0, z$ $0, z, \bar{y}$ $0, z, y$ $0, \bar{z}, \bar{y}$ $0, \bar{z}, y$ $z, y, 0$ $z, \bar{y}, 0$ $\bar{z}, y, 0$ $\bar{z}, \bar{y}, 0$				
48	*i*	*m* .*m* 2	$\frac{1}{2}, y, y$ $\frac{1}{2}, \bar{y}, y$ $\frac{1}{2}, y, \bar{y}$ $\frac{1}{2}, \bar{y}, \bar{y}$ $y, \frac{1}{2}, y$ $y, \frac{1}{2}, \bar{y}$ $\bar{y}, \frac{1}{2}, y$ $\bar{y}, \frac{1}{2}, \bar{y}$ $y, y, \frac{1}{2}$ $\bar{y}, y, \frac{1}{2}$ $y, \bar{y}, \frac{1}{2}$ $\bar{y}, \bar{y}, \frac{1}{2}$				
48	*h*	*m* .*m* 2	$0, y, y$ $0, \bar{y}, y$ $0, y, \bar{y}$ $0, \bar{y}, \bar{y}$ $y, 0, y$ $y, 0, \bar{y}$ $\bar{y}, 0, y$ $\bar{y}, 0, \bar{y}$ $y, y, 0$ $\bar{y}, y, 0$ $y, \bar{y}, 0$ $\bar{y}, \bar{y}, 0$				
48	g	2 .*m m*	$x, \frac{1}{4}, \frac{1}{4}$ $\bar{x}, \frac{3}{4}, \frac{1}{4}$ $\frac{1}{4}, x, \frac{1}{4}$ $\frac{1}{4}, \bar{x}, \frac{3}{4}$ $\frac{1}{4}, \frac{1}{4}, x$ $\frac{3}{4}, \frac{1}{4}, \bar{x}$ $\frac{1}{4}, x, \frac{3}{4}$ $\frac{3}{4}, \bar{x}, \frac{3}{4}$ $x, \frac{1}{4}, \frac{3}{4}$ $\bar{x}, \frac{1}{4}, \frac{1}{4}$ $\frac{1}{4}, \frac{1}{4}, \bar{x}$ $\frac{1}{4}, \frac{3}{4}, x$				
32	*f*	. 3*m*	x, x, x $\bar{x}, \bar{x}, x$ $\bar{x}, x, \bar{x}$ $x, \bar{x}, \bar{x}$ $x, x, \bar{x}$ $\bar{x}, \bar{x}, \bar{x}$ $x, \bar{x}, x$ $\bar{x}, x, x$				
24	*e*	4*m* .*m*	$x, 0, 0$ $\bar{x}, 0, 0$ $0, x, 0$ $0, \bar{x}, 0$ $0, 0, x$ $0, 0, \bar{x}$				
24	*d*	*m* .*m m*	$0, \frac{1}{4}, \frac{1}{4}$ $0, \frac{3}{4}, \frac{1}{4}$ $\frac{1}{4}, 0, \frac{1}{4}$ $\frac{1}{4}, 0, \frac{3}{4}$ $\frac{1}{4}, \frac{1}{4}, 0$ $\frac{3}{4}, \frac{1}{4}, 0$				
8	*c*	$\bar{4}$ 3*m*	$\frac{1}{4}, \frac{1}{4}, \frac{1}{4}$ $\frac{1}{4}, \frac{1}{4}, \frac{3}{4}$				
4	*b*	*m* $\bar{3}$*m*	$\frac{1}{2}, \frac{1}{2}, \frac{1}{2}$				
4	*a*	*m* $\bar{3}$ *m*	$0, 0, 0$				

Table 4.17. The rock salt structure, sodium chloride, B1 .

Formula unit NaCl, sodium chloride

Space group: Fm**3**m (no. 225)

Cell dimensions: a5.6402 Å

Cell contents: 4 formula units

Atomic positions: Na in (4a) m**3**m (0, 0, 0) FCT

Cl in (4b) m**3**m (1/2, 1/2, 1/2) FCT

Examples:

compound	a (Å)	compound	a (Å)	compound	a (Å)	compound	a (Å)
MgO	4.213	MgS	5.200	LiF	4.0270	KF	5.347
CaO	4.8105	CaS	5.6948	LiCl	5.1396	KCl	6.2931
SrO	5.160	SrS	6.020	LiBr	5.5013	KBr	6.5966
BaO	5.539	BaS	6.386	LiI	6.00	KI	7.0655
TiO	4.177	MnS	5.224	LiH	4.083	RbF	5.6516
MnO	4.445	MgSe	5.462	NaF	4.64	RbCl	6.5810
FeO	4.307	CaSe	5.924	NaCl	5.6402	RbBr	6.889
CoO	4.260	SrSe	6.246	NaBr	5.9772	RbI	7.342
NiO	4.1769	BaSe	6.600	NaI	6.473	AgF	4.92

$I\bar{4}c2$ D_{2d}^{10} $\bar{4}m2$ Tetragonal

No. 120 $I\bar{4}c2$ Patterson symmetry $I4/mmm$

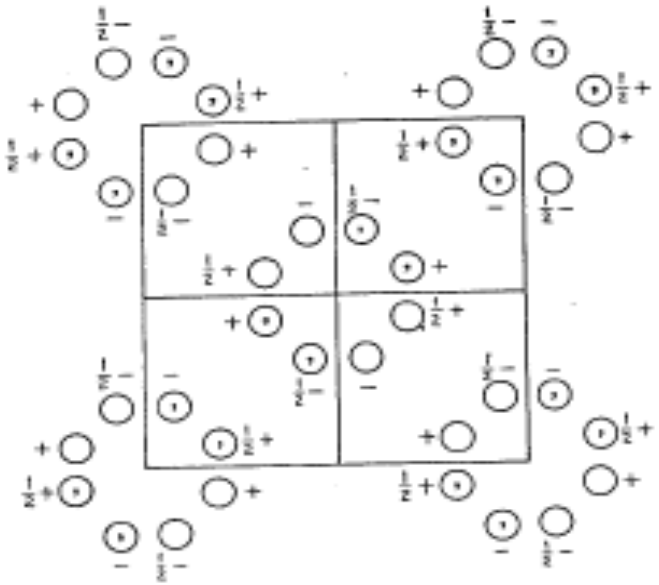

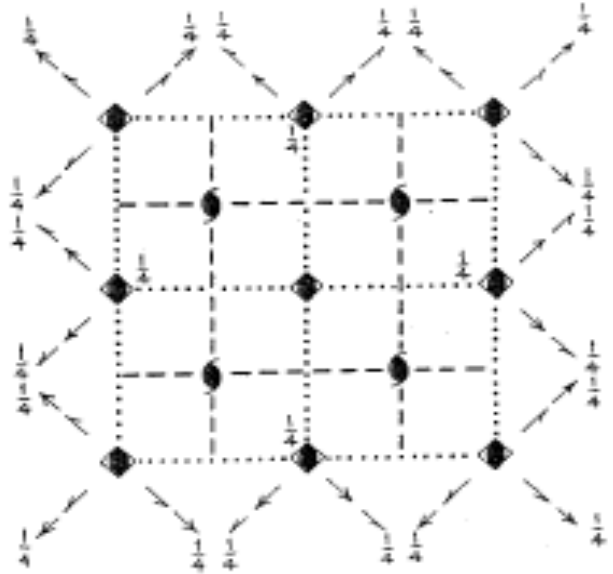

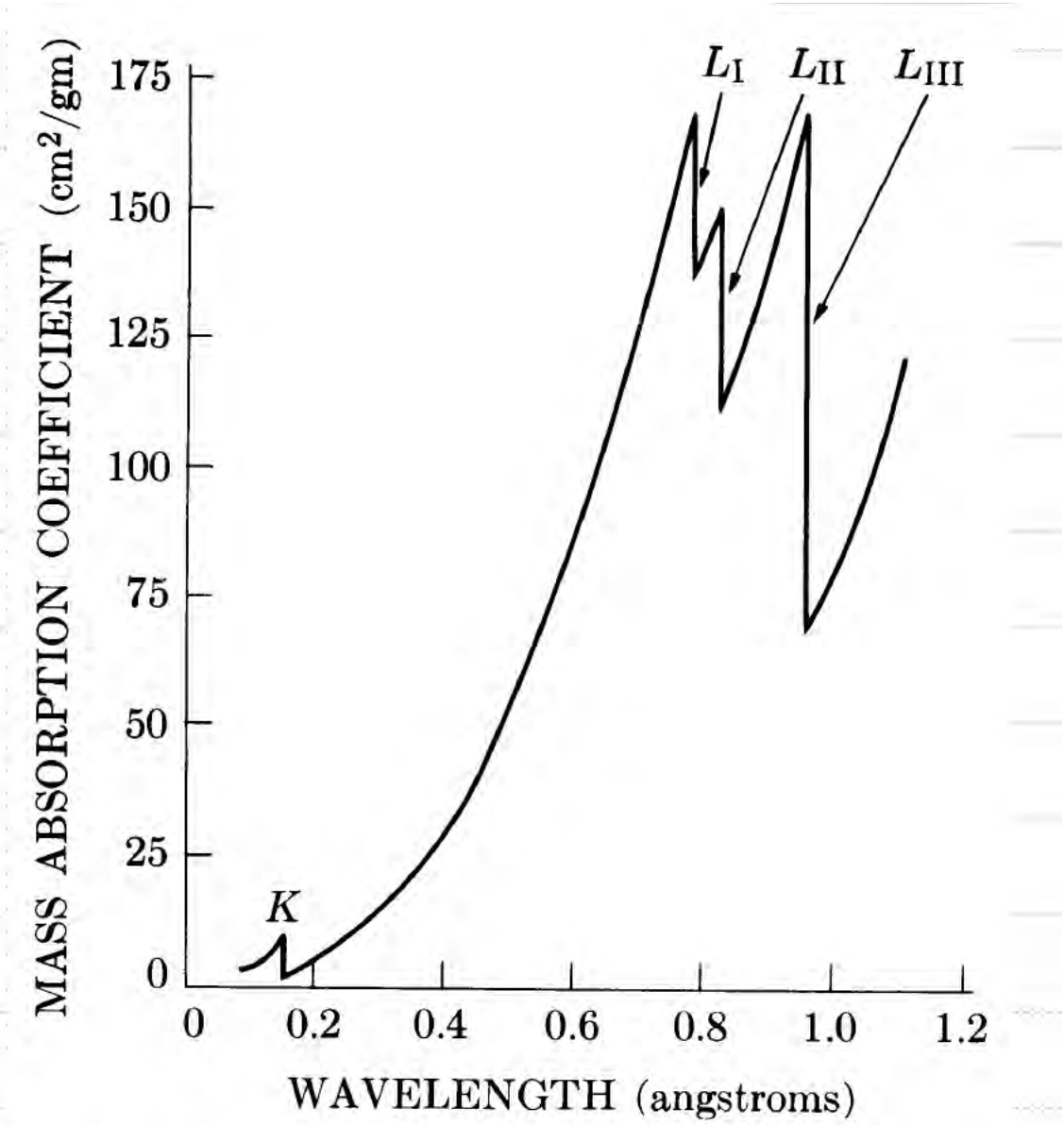

Absorption coefficients of lead

Cu radiation

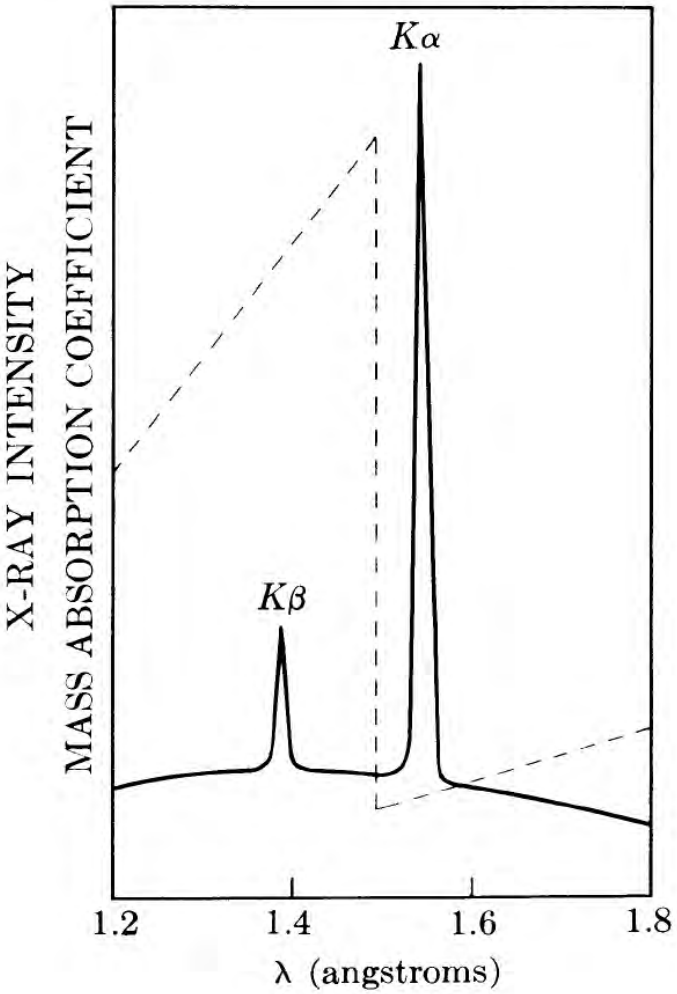

No Filter

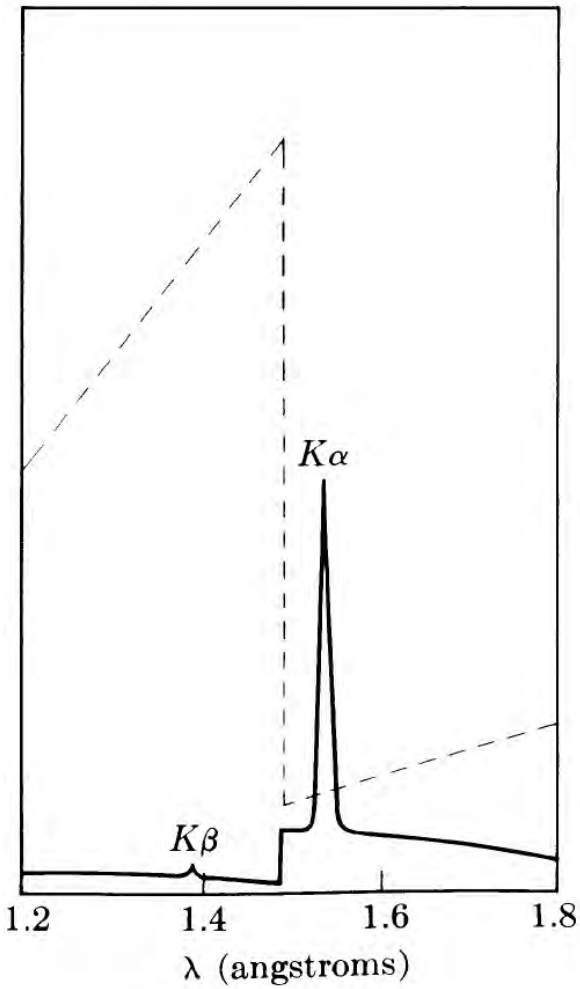

Ni Filter

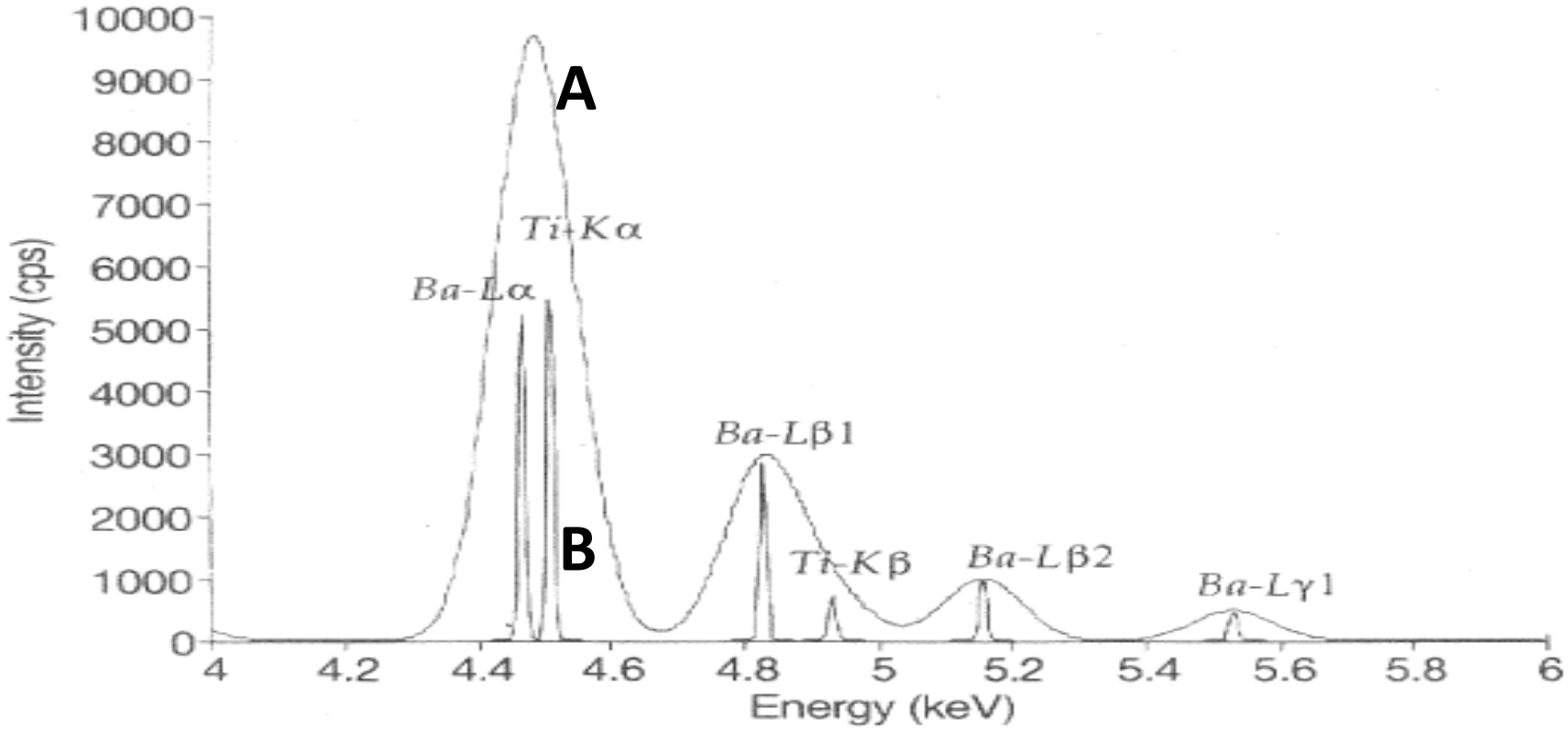

Figure 4 Superposed EDS and WDS spectra from $BaTiO_3$. The EDS spectrum was obtained with a detector having 135-eV resolution, and shows the strongly overlapped Ba $L\alpha_1$–Ti $K\alpha$ and Ba $L\beta_1$–Ti $K\beta$ peaks. The WDS spectrum from the same material shows the peaks to be completely resolved.

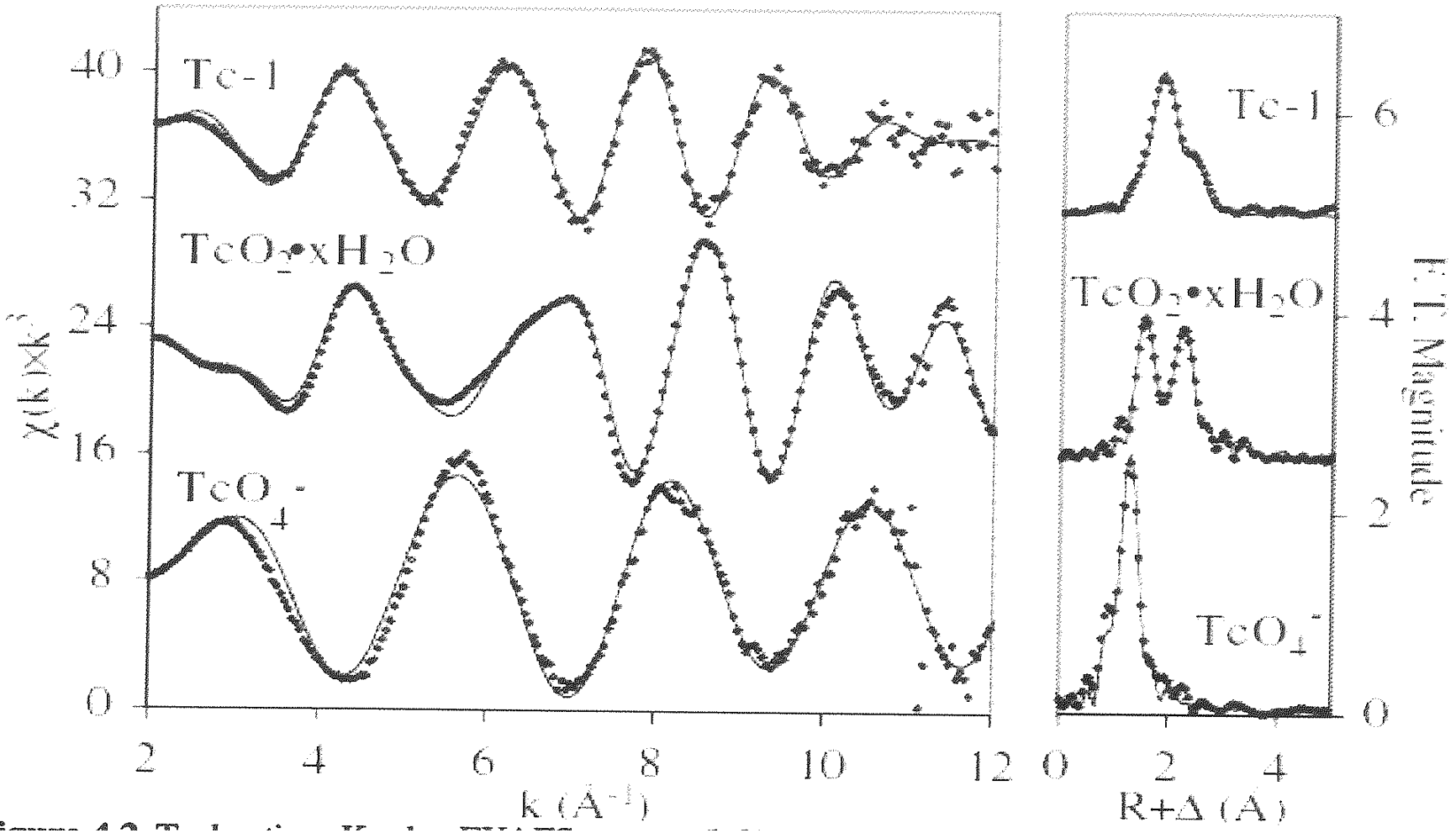
Tc-1
TcO2•xH2O
TcO4-
χ(k)×k2
k (Å-1)
R+Δ (Å)
F.T. Magnitude

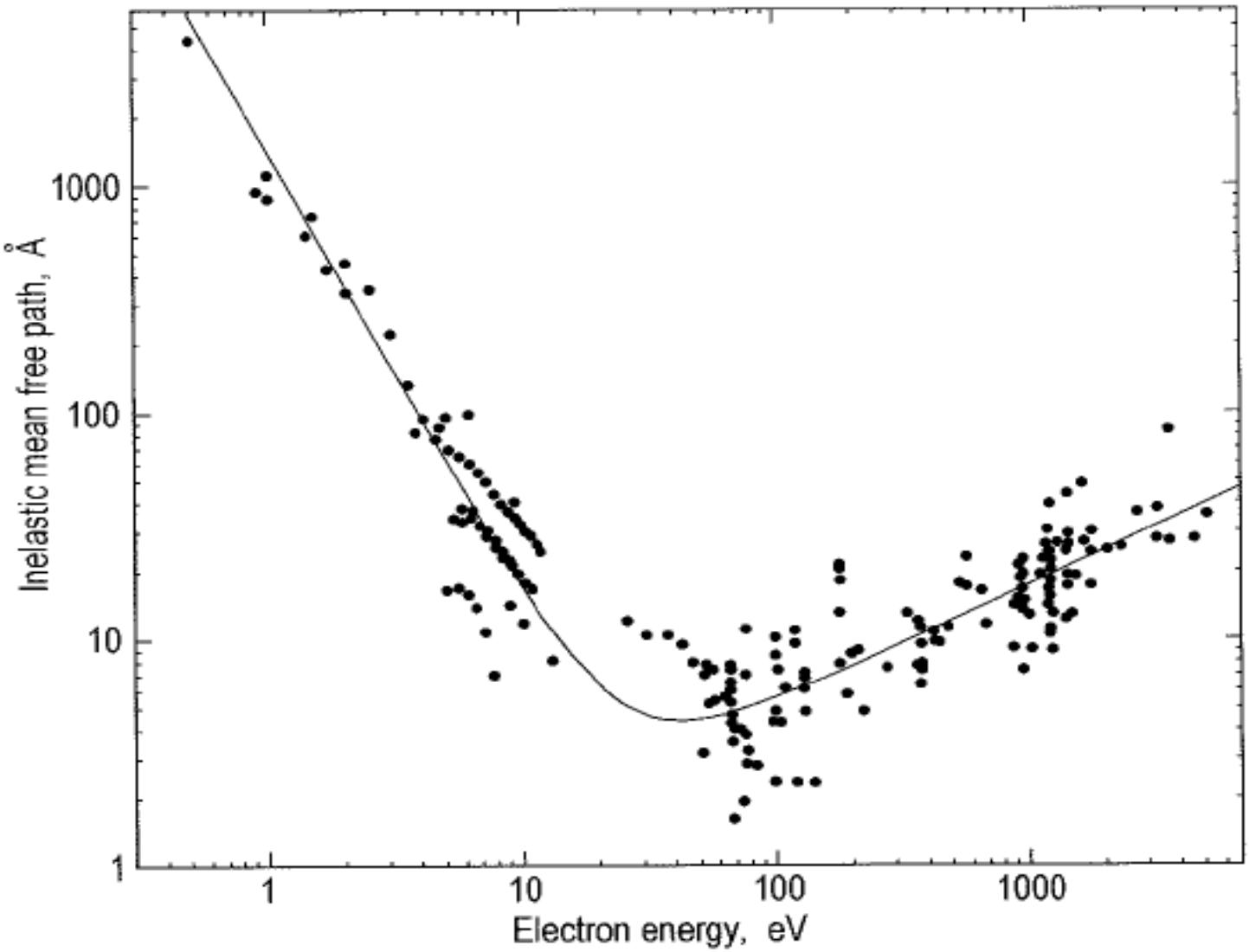
Inelastic mean free path, Å
1000
100
10
1
1
10
100
1000
Electron energy, eV

Silicon, Si Atomic Number 14

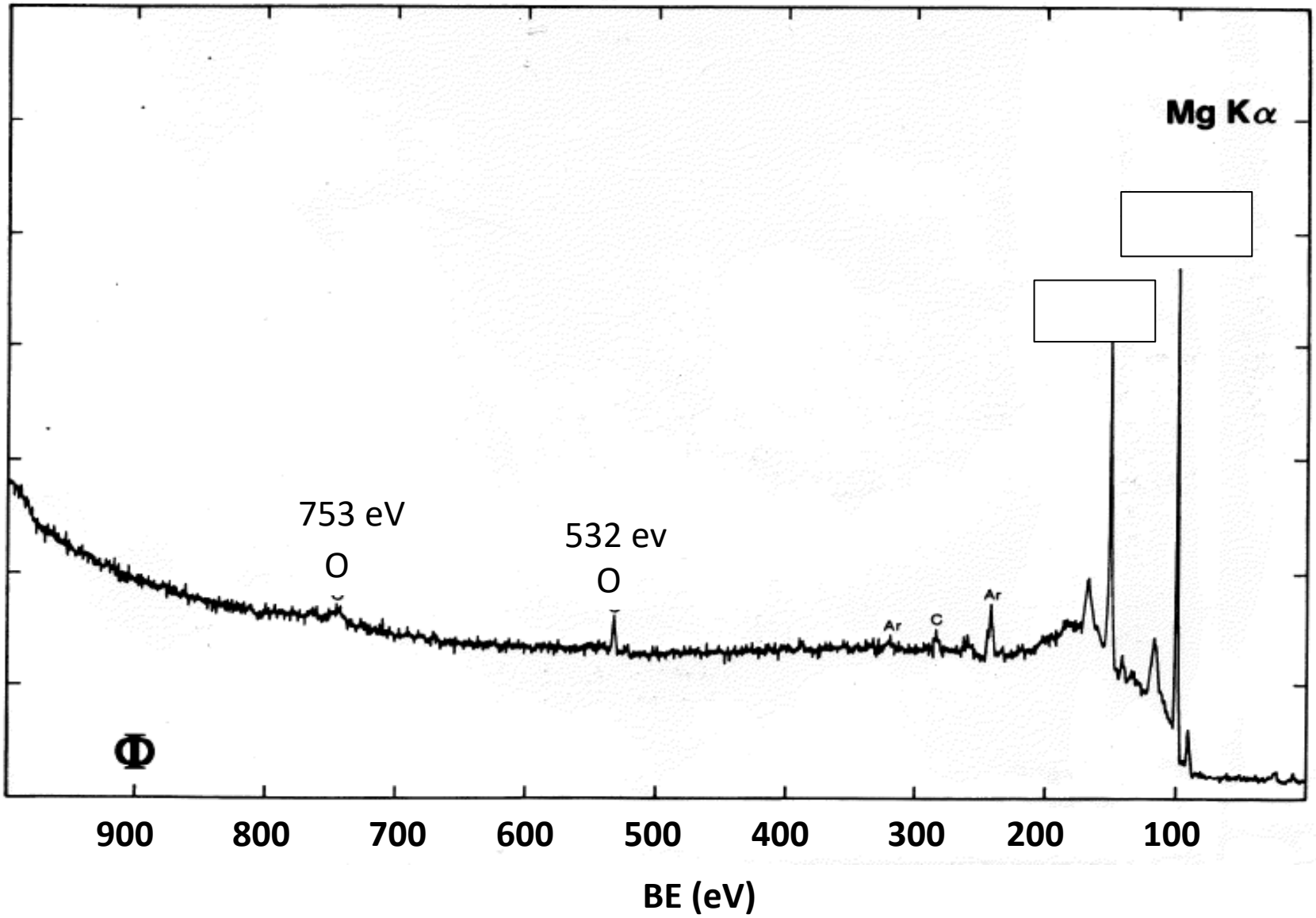

Nickel, Ni Atomic Number 28

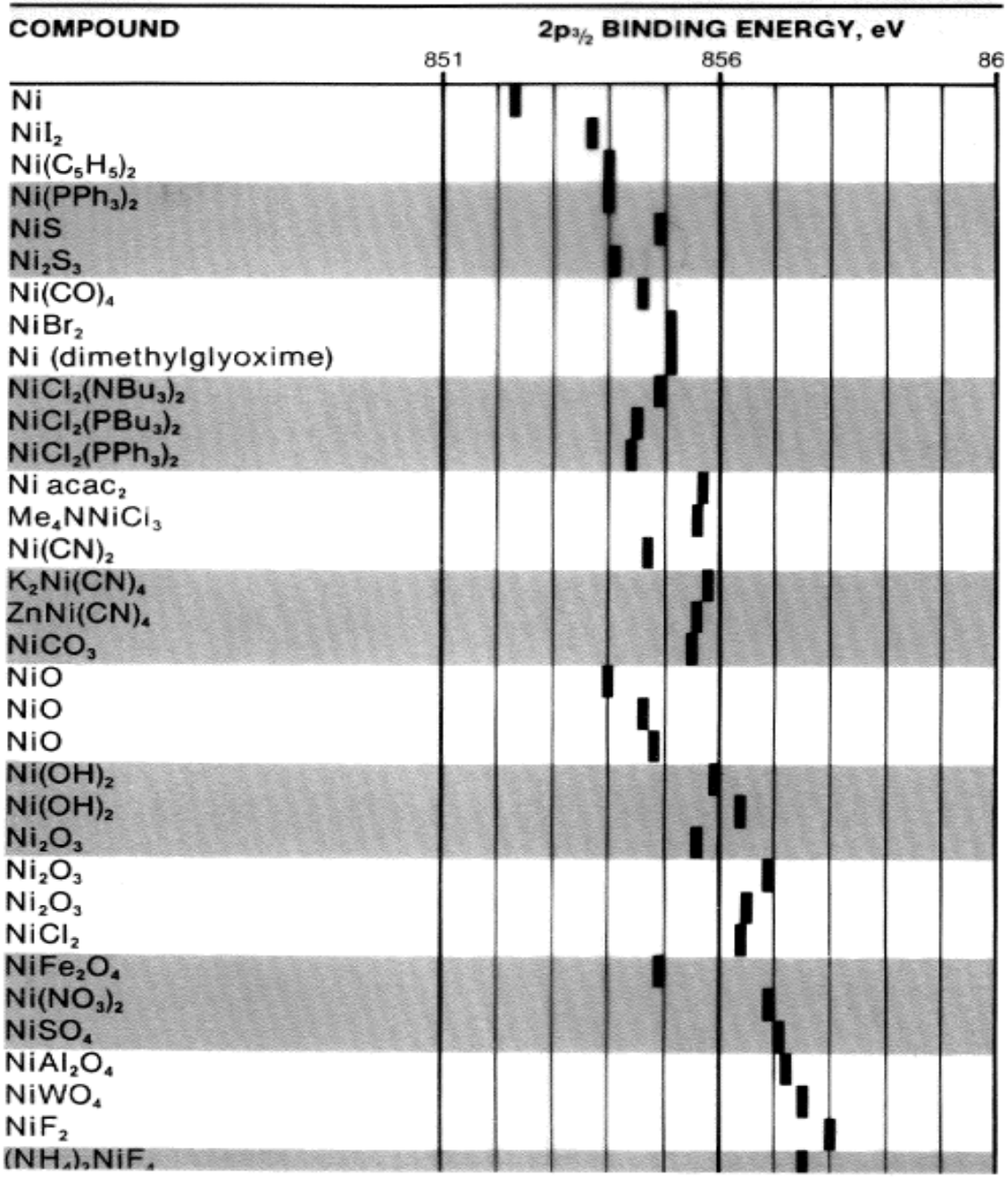

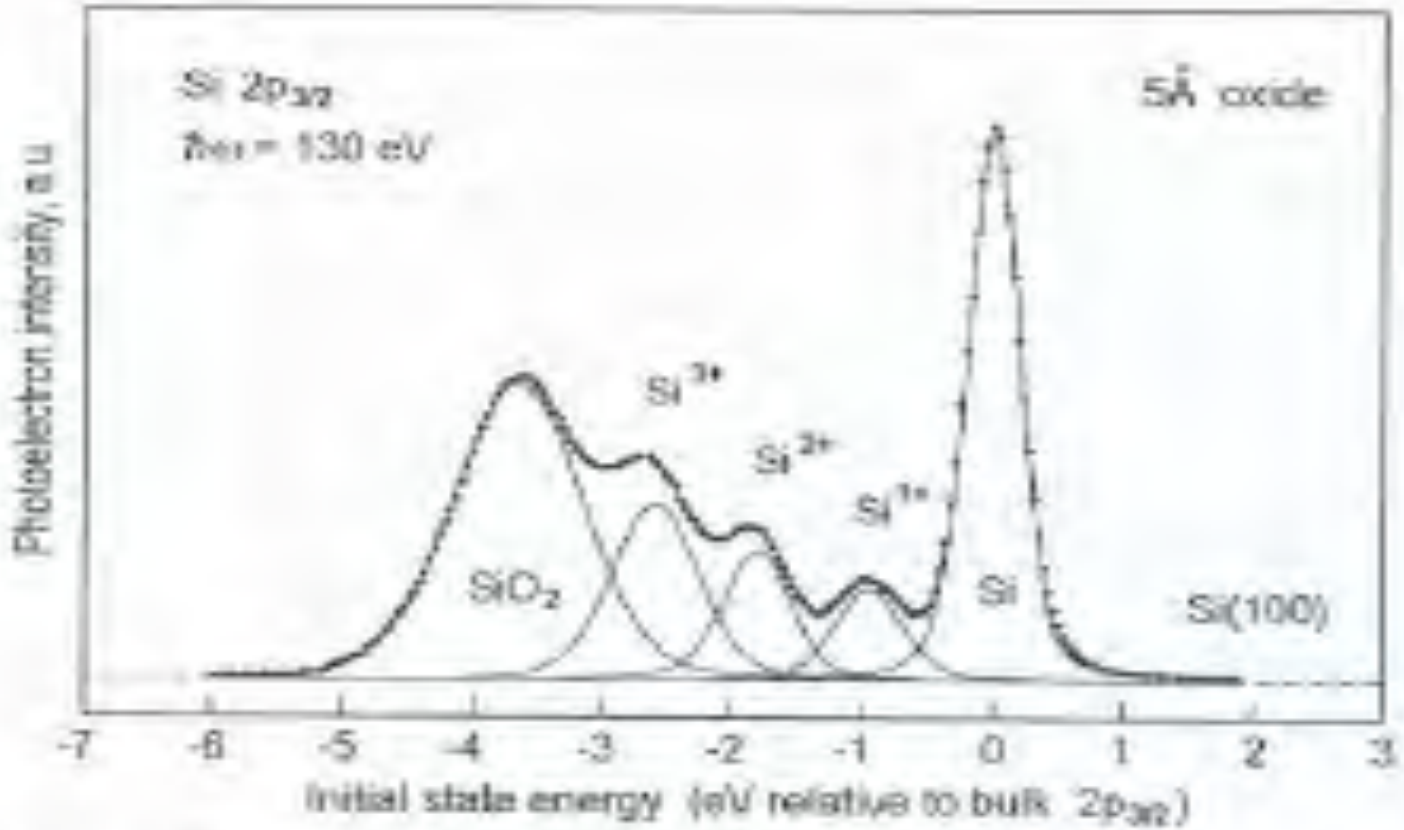

Fig. 5.23. Si $2p_{3/2}$ core-level spectrum from an ultrathin SiO_2 o
Si(100) surface (note that the Si $2p_{1/2}$ partner line is already subtra
the peak due to clean Si, the peaks due Si in different oxides are se
shift to lower energies with increasing oxidation states [after Himpse

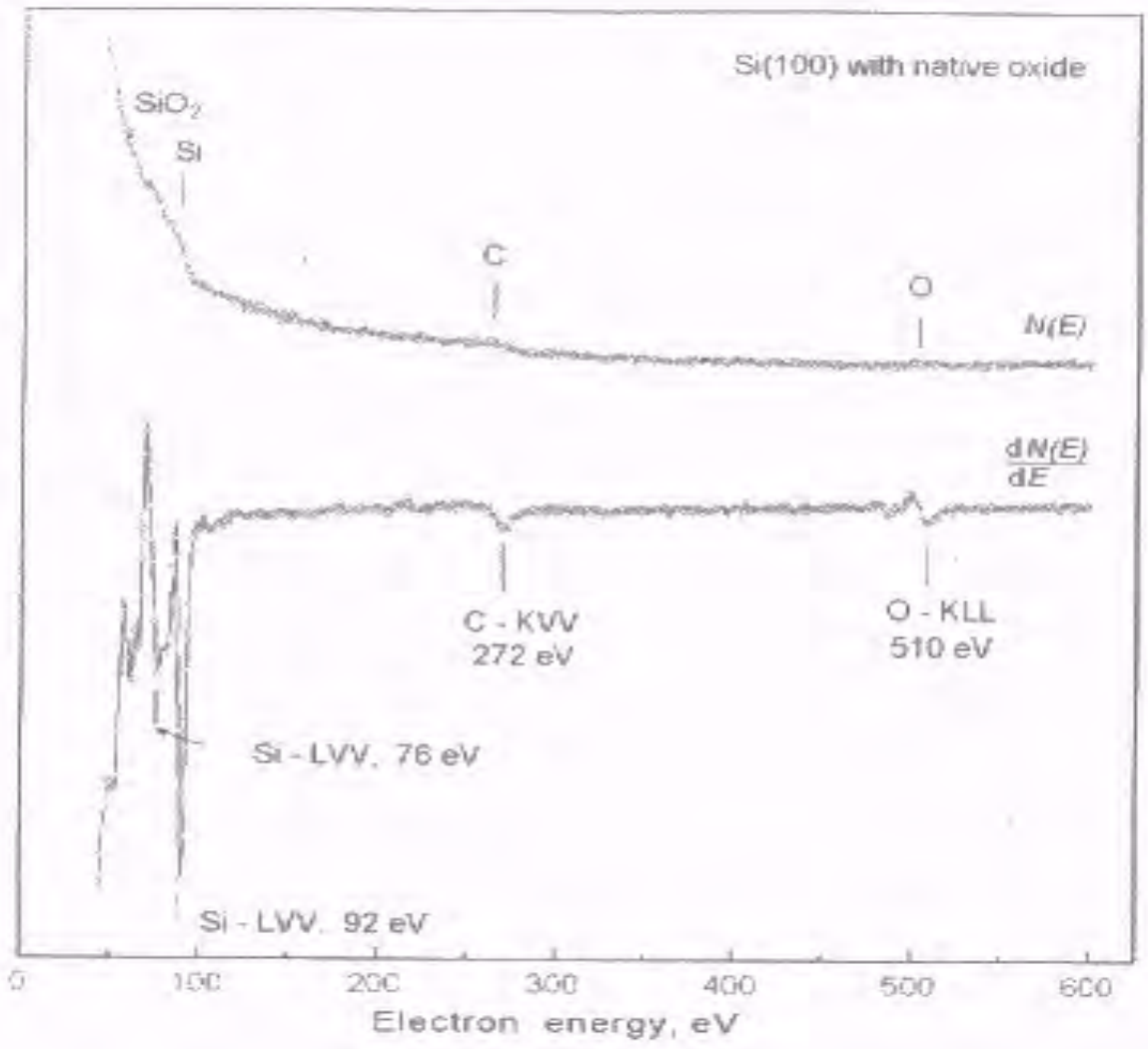
Si(100) with native oxide
SiO2
Si
C
O
N(E)
dN(E)/dE
C - KVV
272 eV
O - KLL
510 eV
Si - LVV, 76 eV
Si - LVV, 92 eV
0
100
200
300
400
500
600
Electron energy, eV

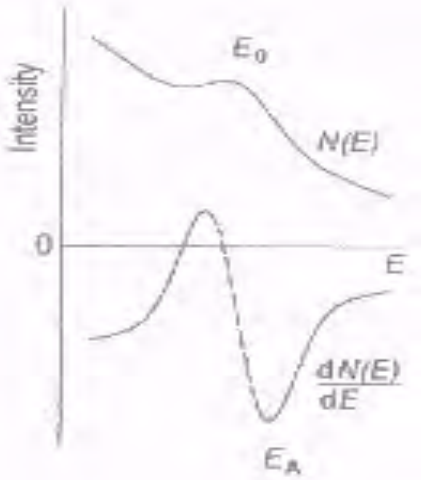
Intensity
E0
N(E)
0
E
dN(E)/dE
EA

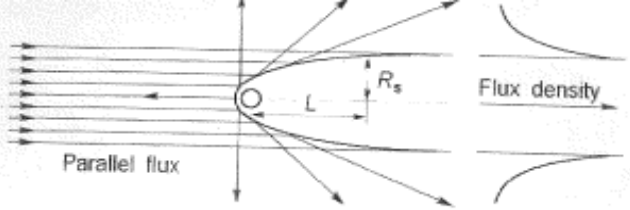

Fig. 6.6. Shadow cone formed from trajectories of projectile ions scattered from a target atom

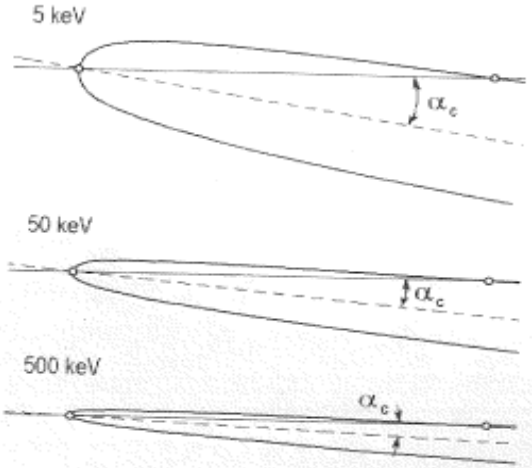

Fig. 6.7. Calculated shadow cones for Li^+ ions with energy of 5 keV, 50 keV, and 500 keV scattering from Ag atoms. The critical angles of shadowing α_c are indicated. The shadow cone width and critical angle decrease substantially with increasing ion kinetic energy (after Williams [6.3])

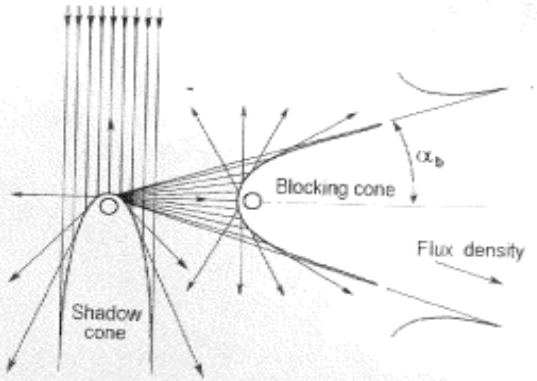

Fig. 6.8. Shadow and blocking cones for scattering from a pair of atoms

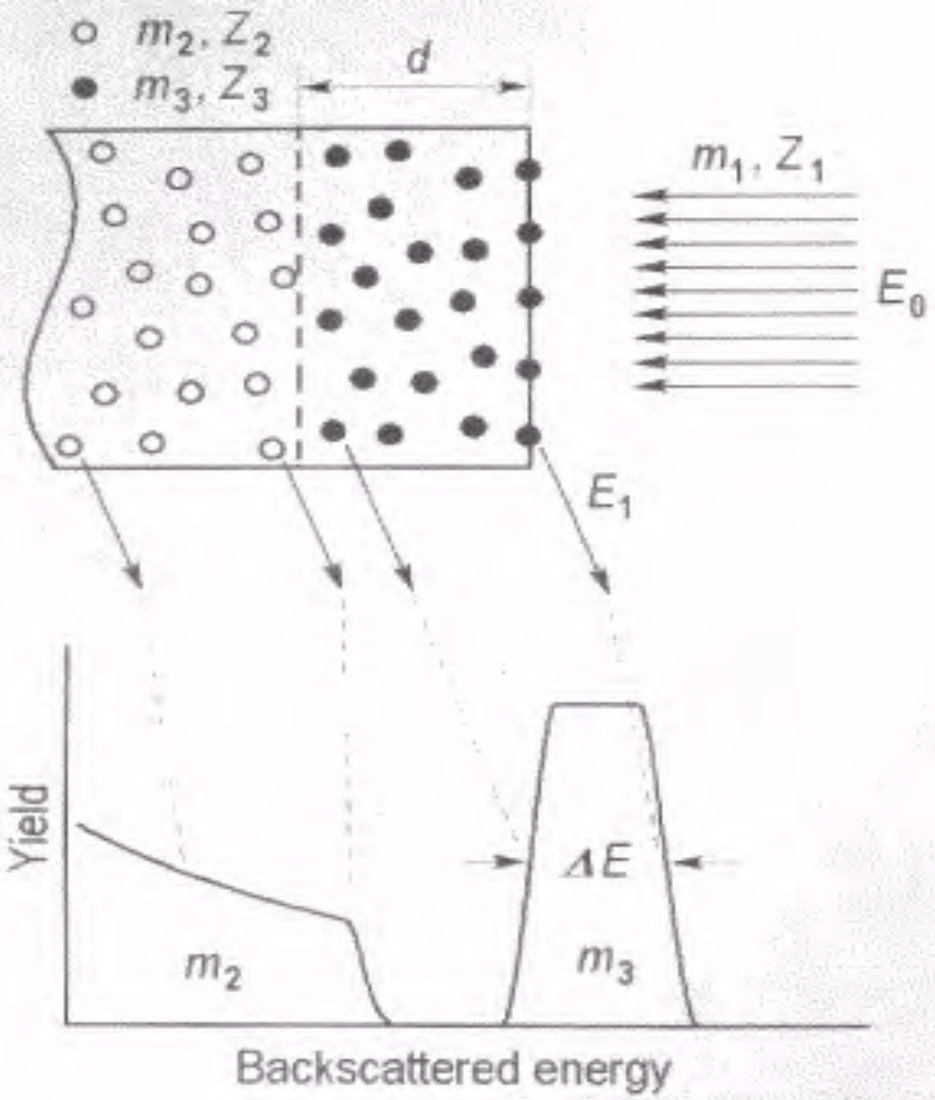

Fig. 6.28. Schematic diagram of the energy spectrum of ions (m_1, Z_1, E_0) scattered from a sample composed of a substrate (m_2, Z_2) and a film (m_3, Z_3) of thickness d. For simplicity, both film and substrate are assumed to be amorphous to neglect the structural effects. (after Feldman et al. [6.6])

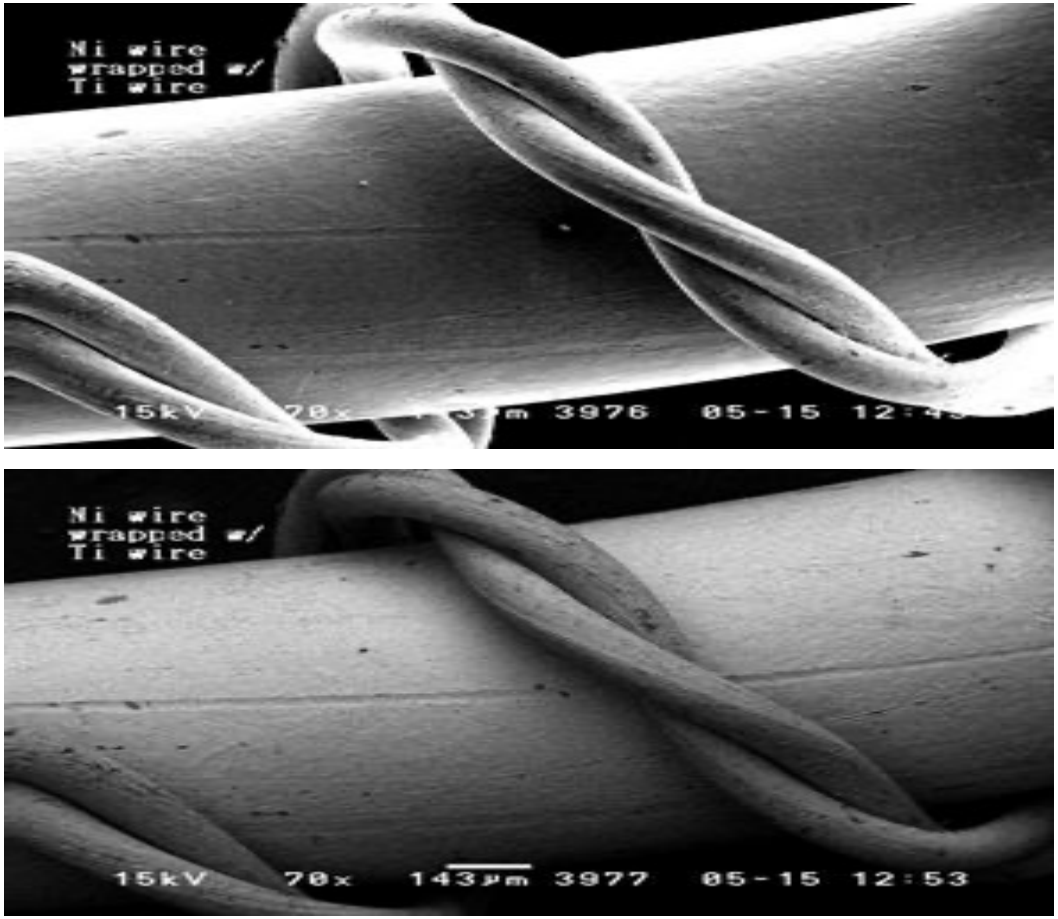

Figure 1: (Top) Secondary electron image of a twisted pair of Ti wires wrapped around a thicker Ni wire is shown. (Bottom) The same specimen is shown in back scatter mode. The two metals can now be differentiated based on contrast; elements of greater atomic mass (Ni in this case) appear brighter in a back scattered electron image. Both images were collected at magnification 70x and show the advantage of great depth of focal field in a SEM.

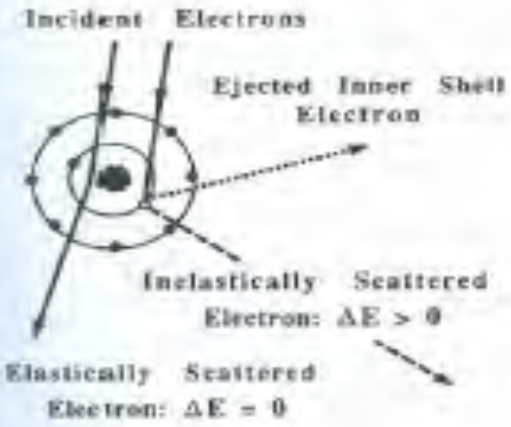

b

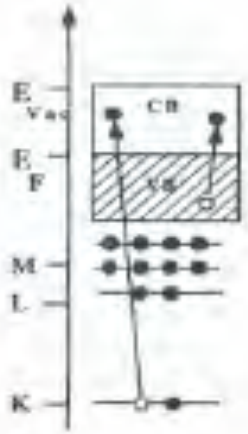

gure 1 (a) Excitation of inner shells by Coulombic interactions. (b) Energy level diagram illustrating excitation from inner shell and valence band into the conduction band and the creation of a corresponding vacancy.

EELS mechanism

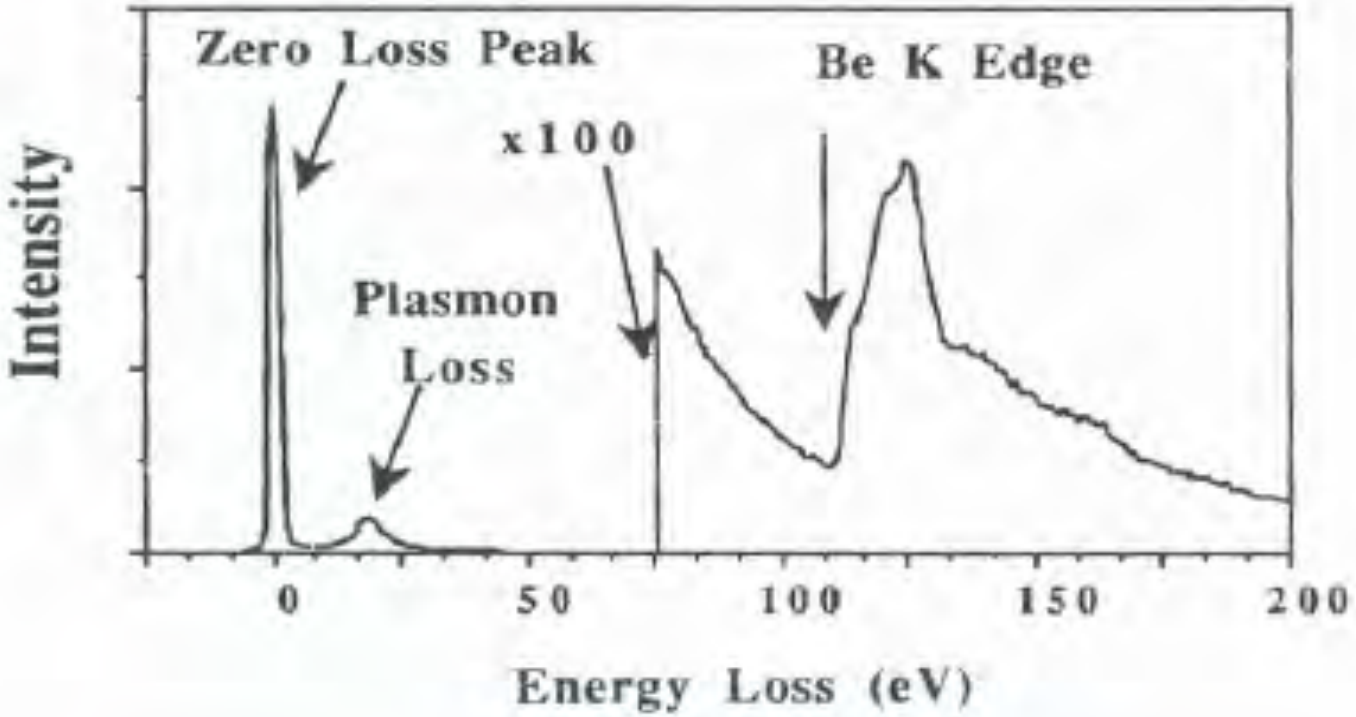
Zero Loss Peak
Be K Edge
x100
Plasmon
Loss
Intensity
0
50
100
150
200
Energy Loss (eV)

EELS

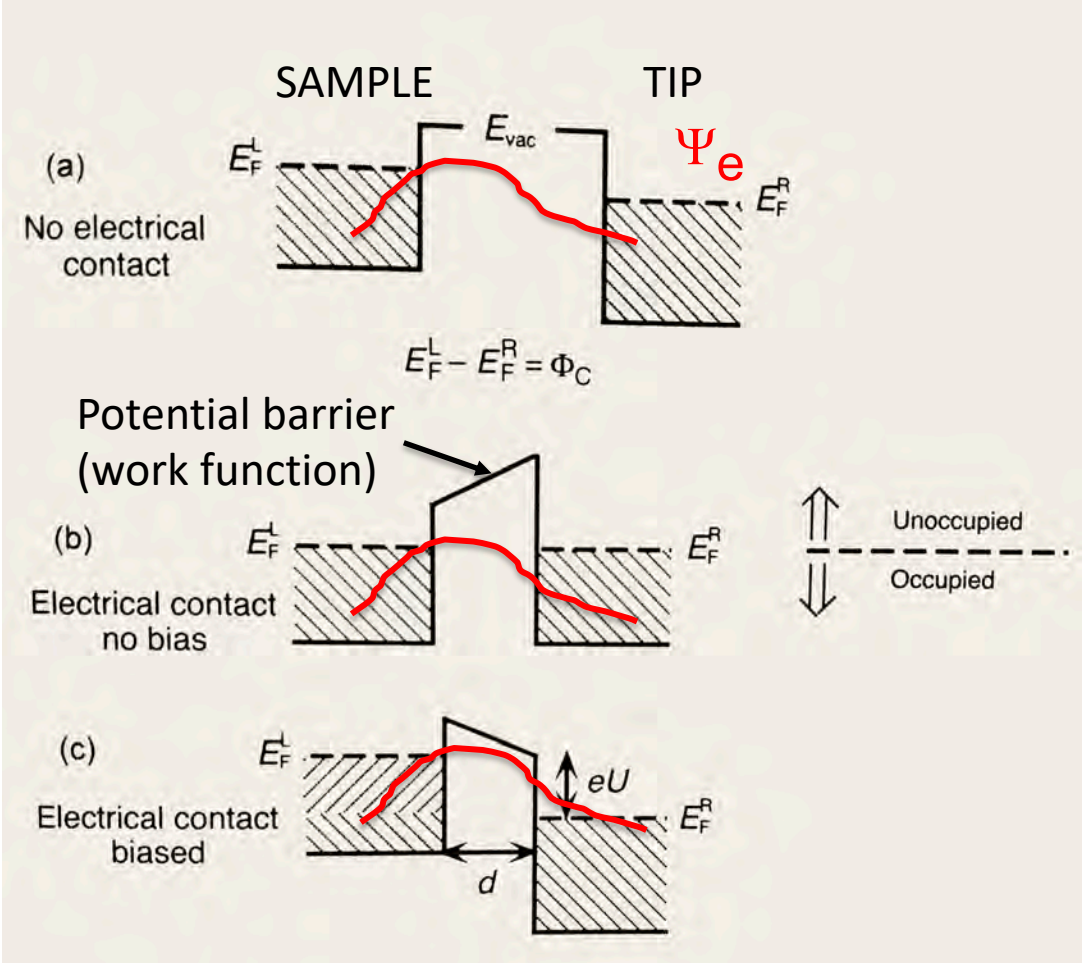

(a) with no elec contact, get different fermi levels for 2 metals (contact potential = Φc). Work functions shown as E_{vac}. Notice work func on tip is larger here.

(b) electrical contact, fermi levels are equal and still higher work func on tip which acts as a barrier to electron migration.

(c) with bias so that tip lower (more+) by voltage U (we use V, so eV). Fermi level in sample higher than tip, so electrons in sample (right slanted lines) can lower energy by moving to tip, but still that solid line=work function barrier exists. But electrons tunnel from sample to tip because of wave function of the electrons.

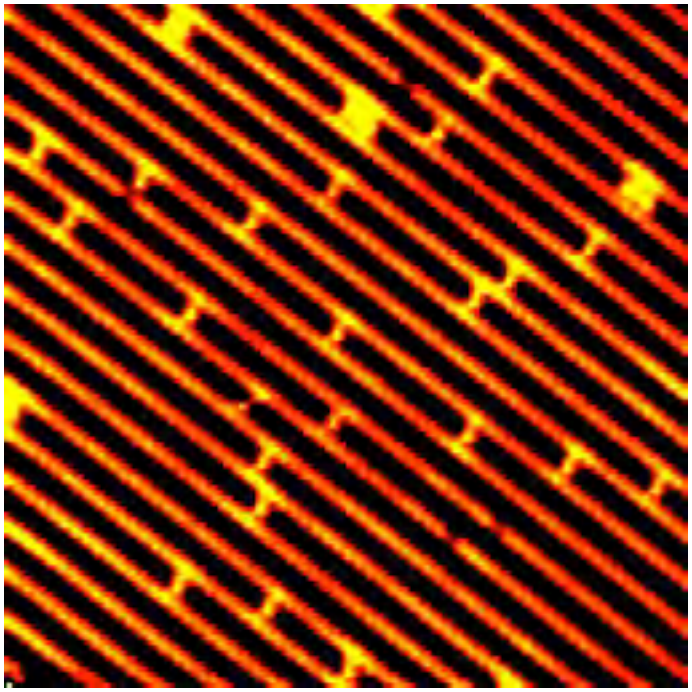

AFM tip

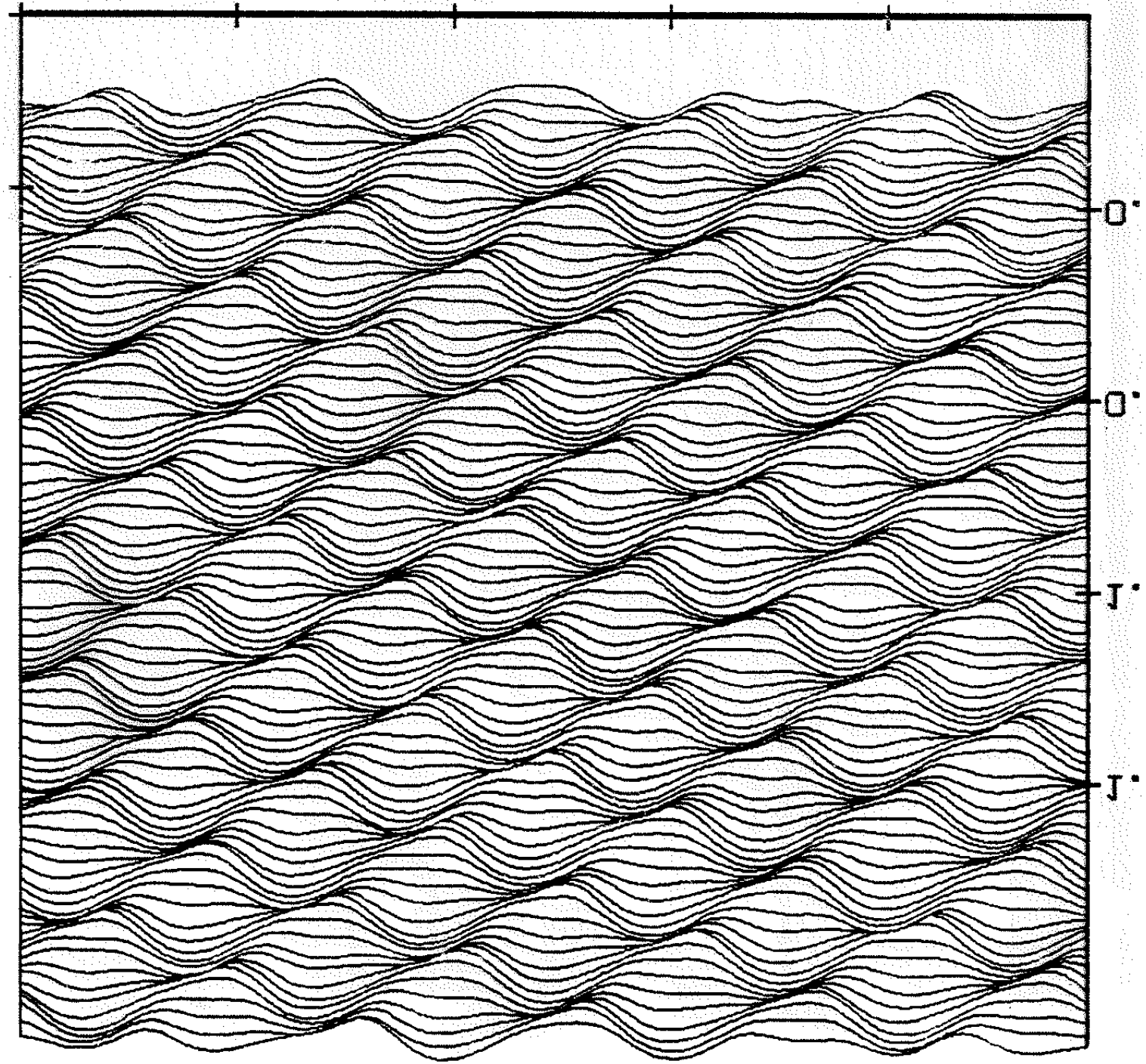
0°
0°
1°
1°

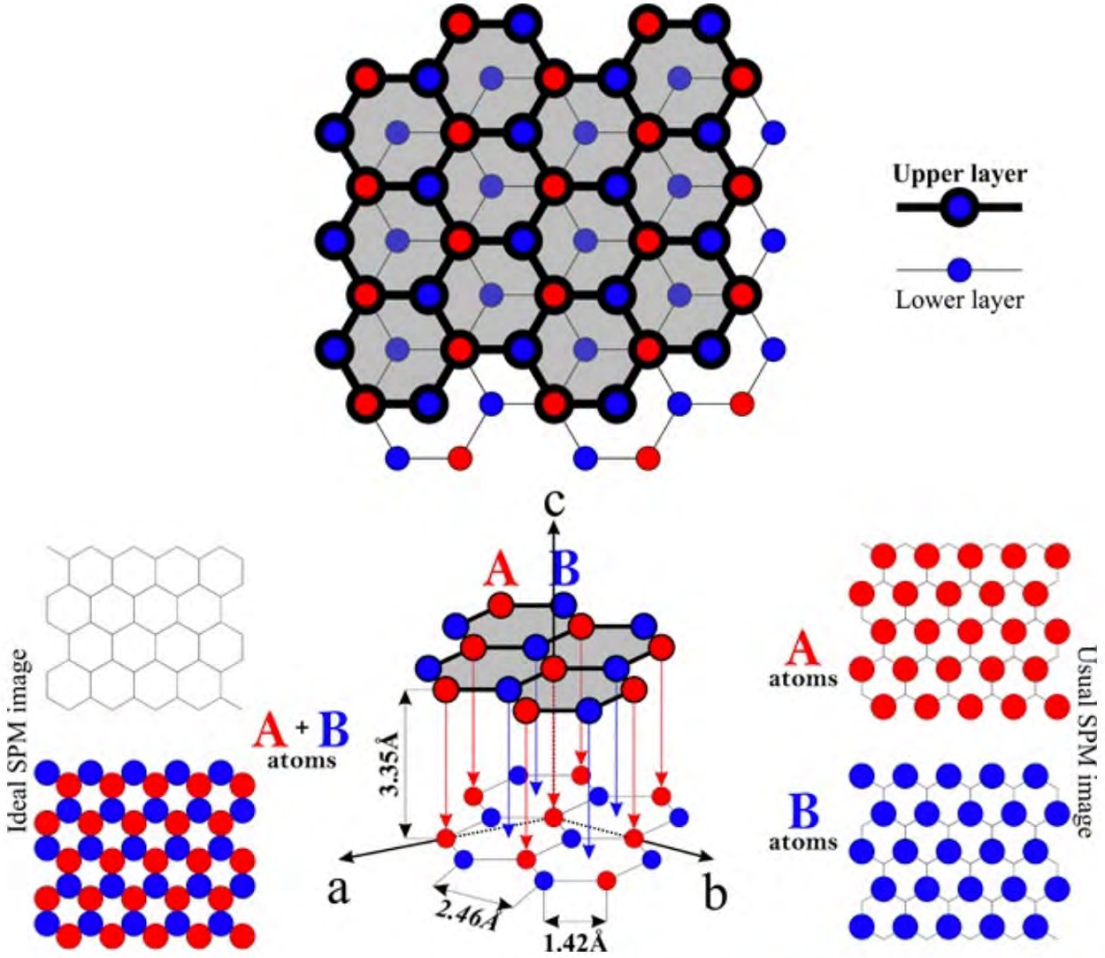

Copied from: http://nanoprobes.aist-nt.com/apps/HOPG%20info.htm

6 carbons in a ring can be classified into 3 A (α) and a B (β) atoms according to their positions relative the lower layer of graphene. B (β) atoms , not sitting atop an atom underneath, gives high tunneling current（"visible"）when imaged under constant height mode, as seen from above result.

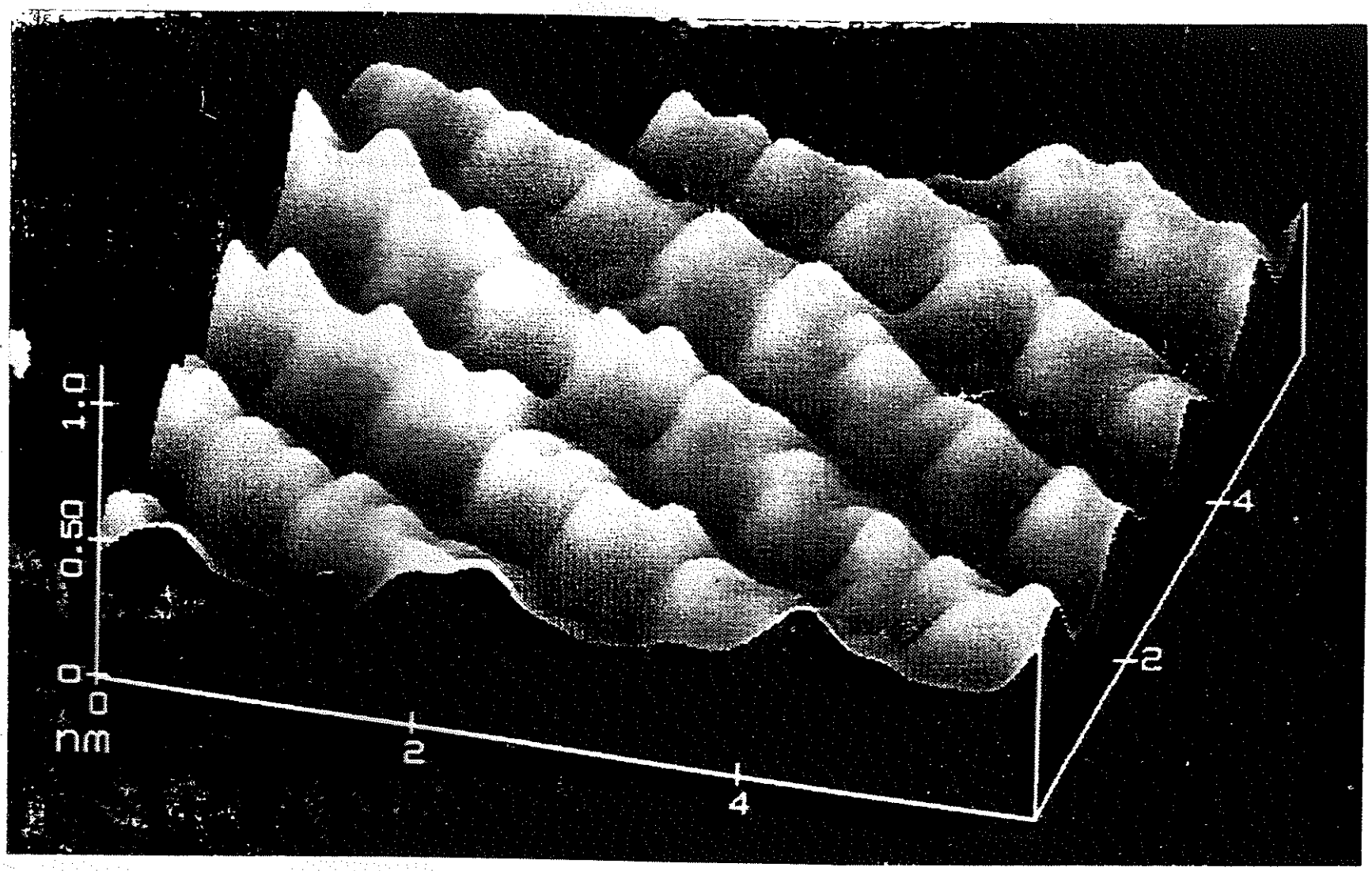

Figure 38.1 STM image of rows of molybdena octahedra on $Rb_{0.3}Mo_{0.7}O_3$, a "molybdenum bronze" (G. Rudd and S. H. Garofalini, Rutgers University, 1992)

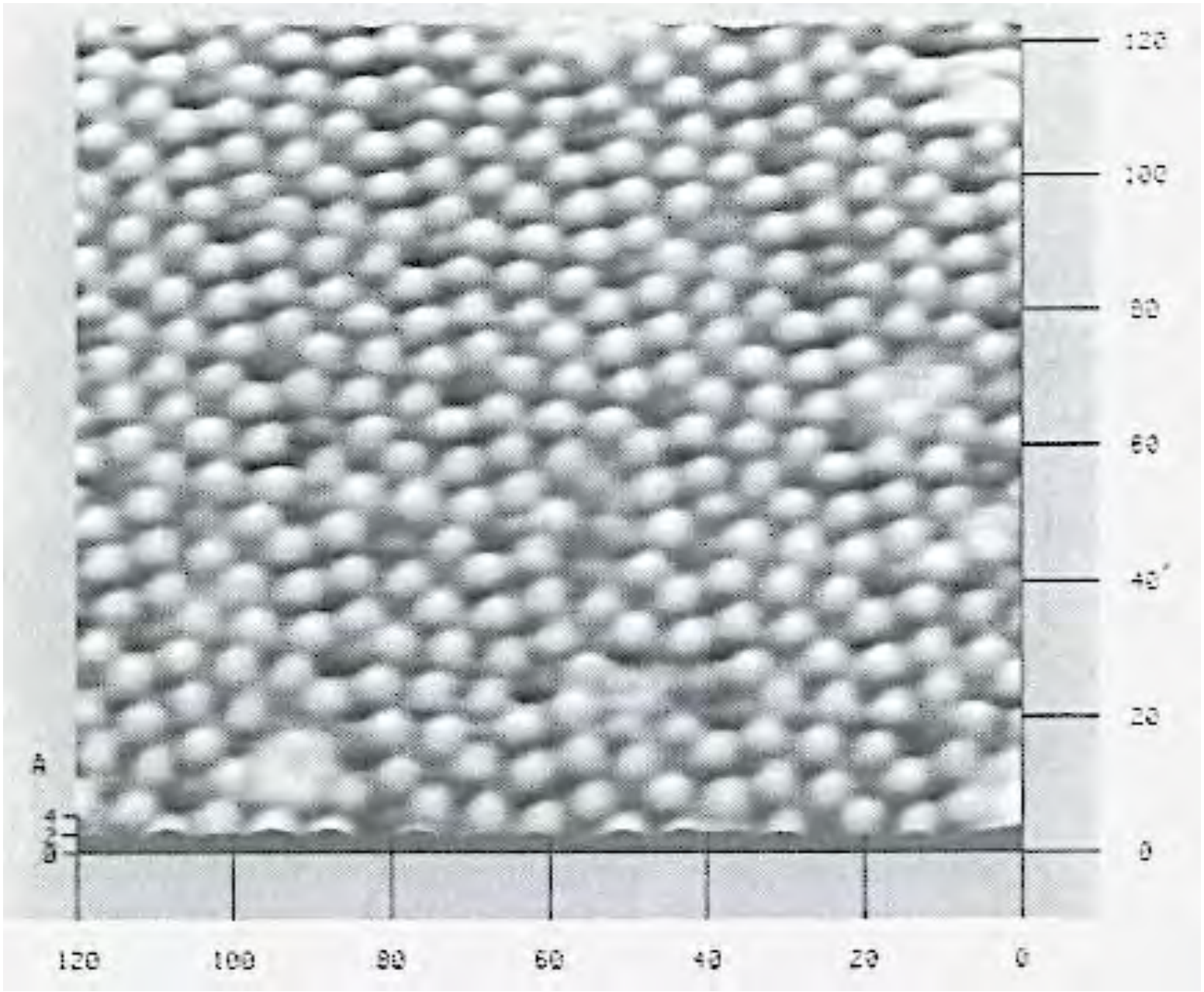
120
100
80
60
40
20
0
120
100
80
60
40
20
0

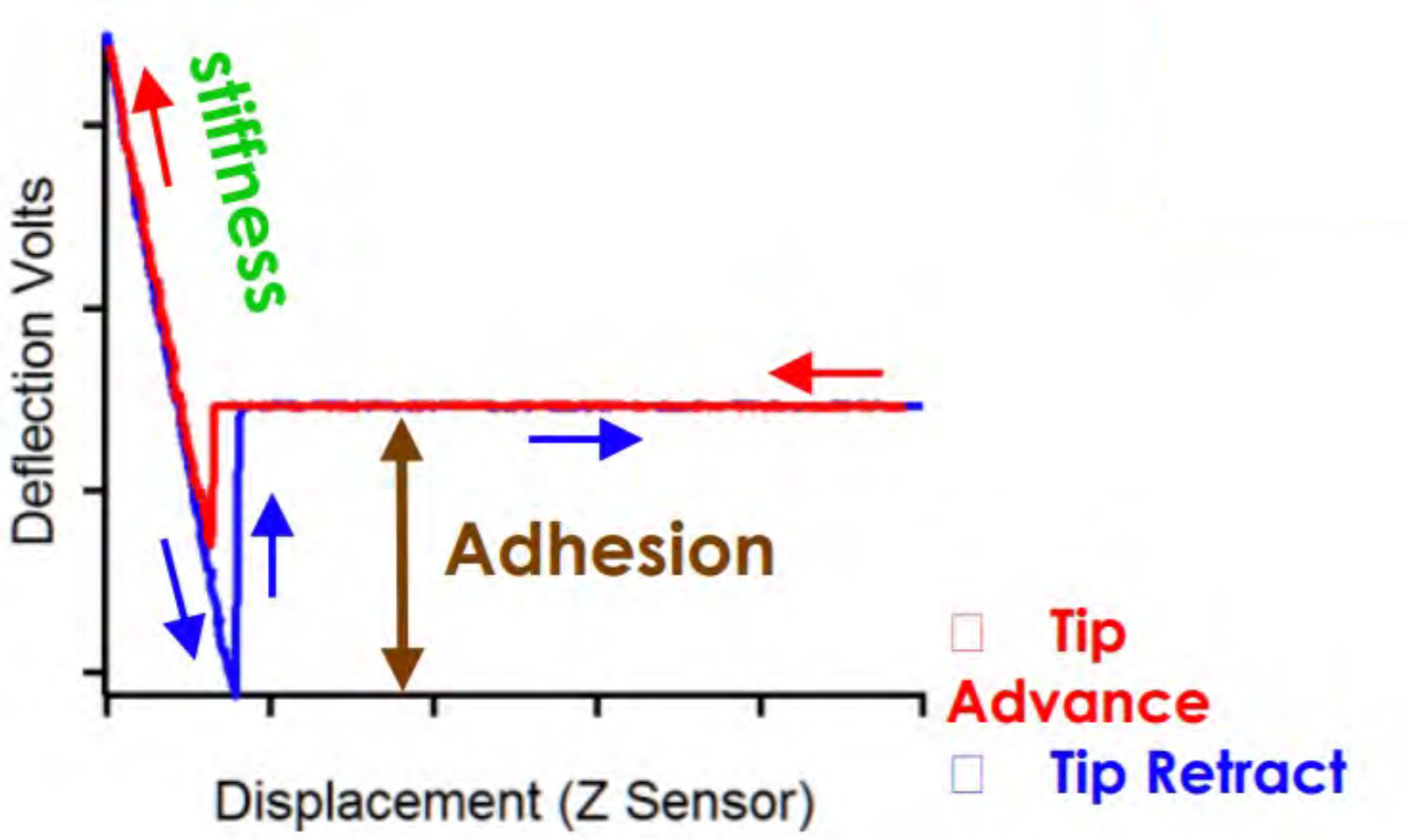
Deflection Volts
stiffness
Adhesion
Displacement (Z Sensor)
Tip Advance
Tip Retract

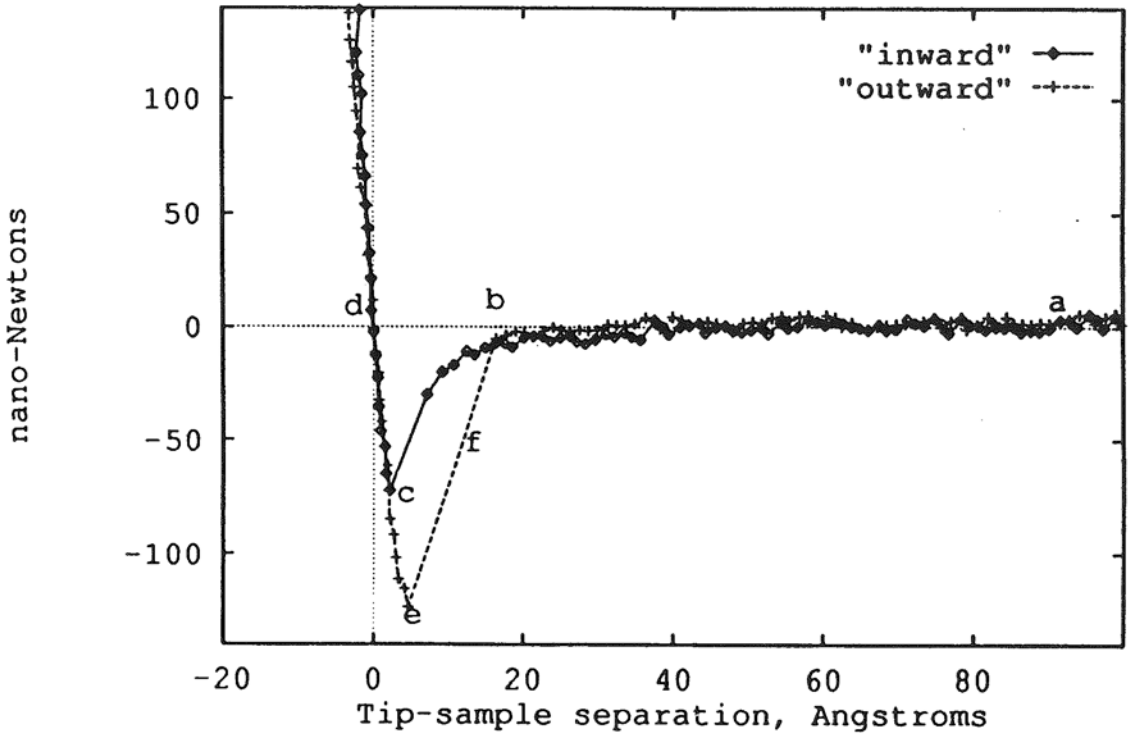

Fig. 1. Example of a *F–D* curve obtained on pure silica under vacuum. Repulsive forces are positive, attractive negative. "Inward" line traces the approach, "outward" withdrawal. At **a**, tip and sample are far apart and no force is measured. Around **b** onset of attraction begins, which is determined from the point where the slope of the attractive force crosses a threshold (about 1 nN/Å). At **c** attractive force reaches a maximum and repulsive forces initiate. At point **d** net force is again zero, and we define this as zero tip–sample separation. On withdrawal, the attractive force goes through a maximum at **e** and is called the "adhesive force." Break-free occurs along **f** and, for discussions in this paper, is the point where the force returns to zero.

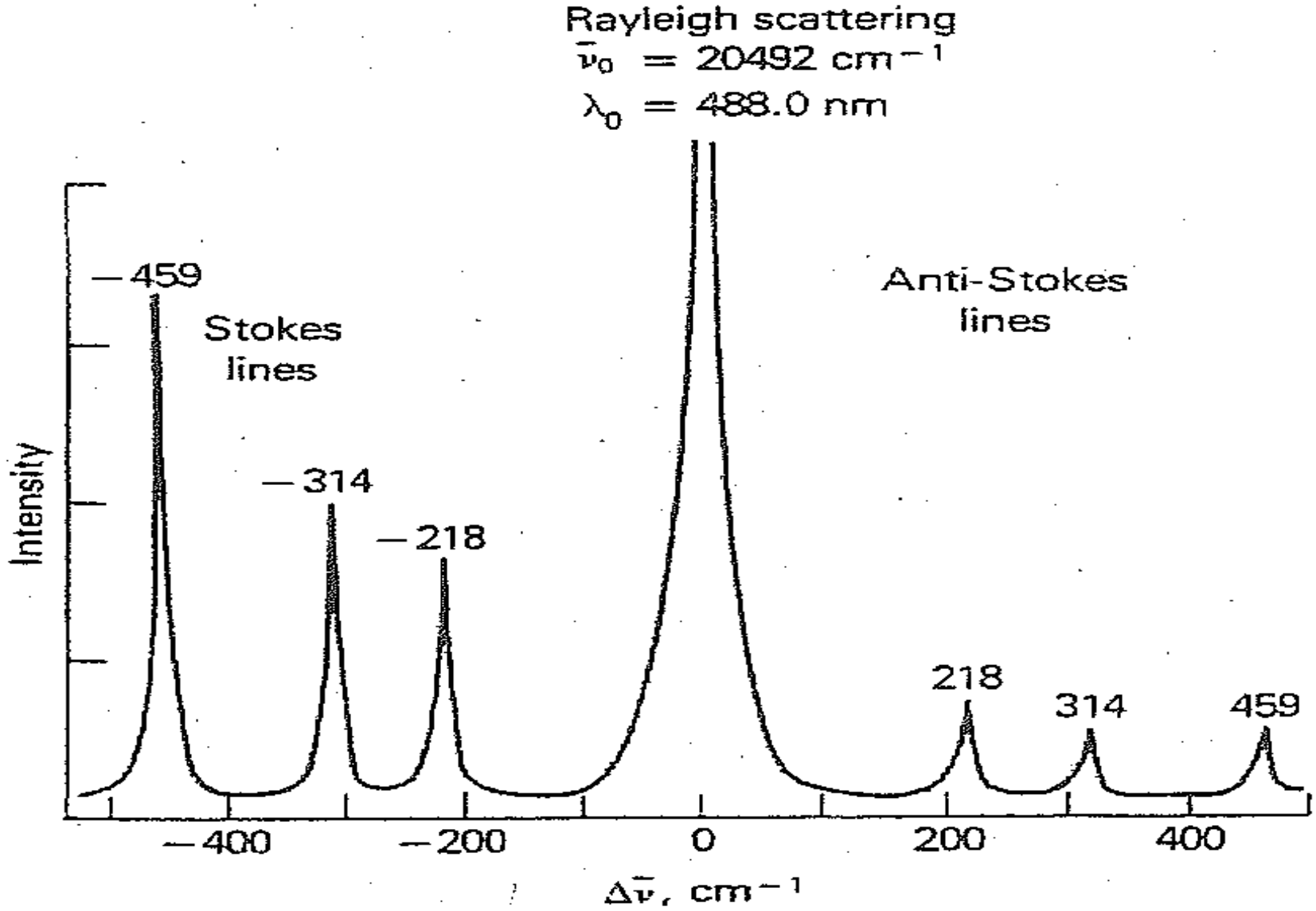

IGURE 13–1 Raman spectrum for CCl_4 excited by lase

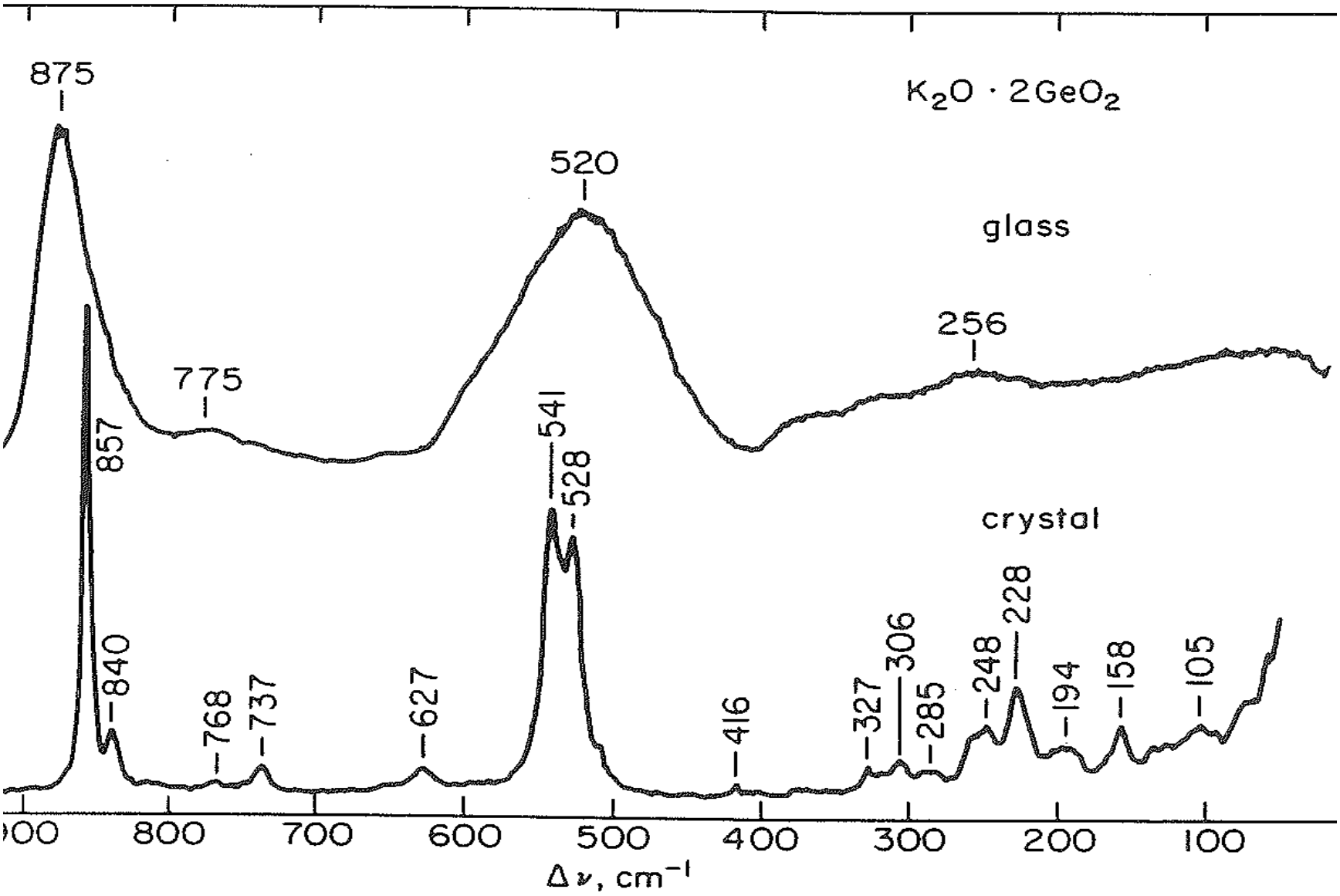

Raman spectra of crystalline and glassy potassium digermanate sho comparison between crystal spectra and glass spectra.